REVISTA DE METALURGIA, 47 (1)
ENERO-FEBRERO, 38-47, 2011
ISSN: 0034-8570
eISSN: 1988-4222
doi: 10.3989/revmetalmadrid.1001

Annealing of a ferritic stainless steel 409 stabilized with titanium and zirconium additions(•)

J.L. Cavazos*, M.P. Guerrero-Mata* and P. Zambrano*

Abstract

A ferritic stainless steel 409 stabilized with titanium and zirconium was subject to thermomechanical processing. It was heated at 1210 °C for one hour, followed by a 75 % hot reduction in three passes, this rolling schedule ended at 980 °C. Samples were cooled to 600 °C by water spraying followed by air-cooling. The alloy was pickled, and was reduced 80 % by cold rolling. The alloy was annealed at different temperatures for 105 s. Additional annealing treatments were carried out at temperatures of 800, 850 and 900 °C for different times. Mechanical testing and texture were made to corroborate the degree of annealing and formability. Mechanical properties and Texture analyses showed that the alloy annealed at 850 °C for 14 min was both completely recrystallized and a very good formability.

Keywords

Ferritic stainless steel; Stabilized; Texture; Zr.

Recocido de una aleación de acero inoxidable ferrítico 409 estabilizado con adiciones de titanio y zirconio

Resumen

Un acero inoxidable ferrítico 409 estabilizado con titanio y zirconio fue sujeto a procesos termomecánicos. El acero fue calentado a 1210 °C durante una hora, seguido por un laminado en caliente del 75 % en tres pases, el proceso terminó a los 980 °C. Las muestras fueron enfriadas hasta 600 °C por agua atomizada seguido de enfriamiento al aire. La aleación fue decapada y laminada en frío un 80 %. Posteriormente de desarrollaron tratamientos térmicos de recocido a diferentes temperaturas por un tiempo de 105 s. Adicionalmente se desarrollaron tratamientos de recocido a temperaturas de 800, 850 y 900 °C a diferentes tiempos. Pruebas mecánicas y textura fueron realizadas para corroborar el grado de recocido y su formalidad. El análisis de las propiedades mecánicas y la Textura mostraron que la aleación recocida a 850 °C por 14 min (840 s) fue completamente recristalizada obteniendo la mejor formabilidad.

Palabras clave

Acero inoxidable ferrítico; Estabilizado; Textura; Zr.

1. INTRODUCTION

Ferritic stainless steels are alloys of iron and chromium containing 15 - 30 % Cr with additions of Mo, Mn, Si, Al, Nb, Ti, and essentially free from nickel. Table I shows typical compositions of these alloys, particularly one of the most used for catalytic exhaust systems.

The exhaust systems of practically all passenger cars produced in the United States are made from stainless steels. About 23 kg (50.6 lbs) of stainless steels are currently used per vehicle. This level translates to an annual consumption of approximately 400,000 tons of stainless steels in a market of 15 million vehicles per year[1].

Due to increasing restrictions to minimize air pollution, the automotive industry has been requested to guarantee a 10 years lifetime for exhaust systems. Therefore, it is necessary to design new alloys with improved formability and corrosion resistance.

The main problem with stainless steels is sensitization, which is caused by the formation of chromium carbides or nitrides at grain boundaries. This phenomenon leaves a depleted chromium zone around the precipites that makes the steel susceptible to intergranular corrosion. Addition of elements that scavenge carbon and nitrogen rather than chromium solves this problem. The elements that have been found to be most useful are titanium and niobium. When sensitization is

(•) Trabajo recibido el día 12 de enero de 2010 y aceptado en su forma final del día 5 de agosto de 2010.
* Universidad Autónoma de Nuevo León, Facultad de Ingeniería Mecánica y Eléctrica, Avda. Universidad S/N, Cd. Universitaria, San Nicolás de los Garza, Nuevo León, 66450 MEXICO. E-mail: *jose.cavazosgc@uanl.edu.mx.*

controlled, the alloy is fully stabilized. Addition of titanium and niobium increase the corrosion resistance[2], improves formability[3 and 4] and allows weld toughness in the produced steel[5].

A ferritic stainless steel with zirconium and titanium additions was designed to stabilize the alloy; good corrosion resistance and very good formability by thermomecanical processing was obtained[6].

The term texture is used in reference to the distribution of crystal orientations in a polycrystalline aggregate[7 and 8]. In the usual sense, it is a synonymous to a preferred orientation, in which the distribution of crystal orientations is not random. A polycrystalline aggregate with a preferred orientation is anisotropic in nature[9], i.e., it shows different properties in different directions. This dependence of properties on direction could be either beneficial or detrimental, depending upon the intended use of the material. Also, a texture that is beneficial for a particular application could be detrimental in another one. Materials that are designed to be formed are processed to achieve a high value of r_m (normal anisotropy); the ideal crystallographic orientation to maximize r_m in bcc metals would be a sheet texture with <111> in the direction normal to the sheet and {111} oriented randomly in the plane of the sheet[10]. The correct texture gives the proper orientation of slip systems so that the strength in the normal direction (ND) is greater that than in the plane of the sheet. To improve the properties of ferritic stainless steels, one of the factors is to create a desirable texture after cold rolling and annealing for improving deep drawability. That is to develop a strong texture <111> // ND.

The objective of this work is to determinate the adequate temperature and time to obtain a full annealing in a ferritic stainless steel 409 with zirconium and titanium additions to improve the formability. Full annealing will be related by texture analyses and mechanical testing.

2. EXPERIMENTAL PROCEDURE

The chemical composition of the alloy was obtained from laboratory ingots; the results are presented along with the nominal alloy values in table I. The ingots were sectioned into pieces of 25.4 mm (thick) by 76.2 mm (wide) by 101.6 mm (long). A thermocouple was placed into the center of each sample. The specimens were heated at 1210 °C for one hour, followed by a 75 % reduction in three passes (25.4 to 6.35 cm). The temperature at the exit of the first pass was 1160 °C; at the exit the second pass was 1075 °C, and at the exit of the third pass was 980 °C. At this point the alloys were cooled to 600 °C by water spray followed by air-cooling, this schedule was for avoiding martensite formation, no martensite was found after hot rolling. The alloy was pickled in a solution of HCl in water to remove the oxide layer. The material was then reduced 80 % by cold rolling in four passes (6.1 mm to 1.12 mm). Table II shows the rolling schedules.

The samples were annealed at different temperatures in the range from 300 to 900 °C with intervals of 100 °C during 105 s. This procedure is the conventional treatment in a continuous annealing line. Additional heat treatments were made at temperatures of 800, 850 and 900 °C at different times (3.5, 7 and 14 min). The temperatures were measured in the samples using a thermocouple. Microhardness was measured using a load of 500 g for 15 s.

Quantitative metallographic analyses were performed on specimens cut from cold rolled and annealed samples using image analyzer system, to get the average grain size and aspect ratio. A minimum of 300 grains were measured for each specimen to obtain a true picture of the bulk sample and obtain a proper statistical distribution of the grains.

Texture on a local basis was obtained in a scanning electronic microscopy adapted with the TSL

Table I. Chemical Composition for alloy 409 (ASTM 240)[17] and the one selected for this work

Tabla I. Composición Química de la aleación 409 (ASTM 240)[17] y la seleccionada para este trabajo

	C	N	Mn	P	S	Si	Cr	Ni	Ti	Zr	Ta
Nominal	0.08 max.	—-	1.00 max.	0.045 max.	0.030 max.	1.00 max.	10.5-11.75	0.50 max.	6xCmin. 0.75 max.	—-	—-
This Work	0.021	0.02	0.13	—-	—-	0.39	11.73	0.15	0.12	0.15	0.016

Table II. Rolling schedules

Tabla II. Plan de Laminado

Hot Rolling
Laminado en Caliente

Pass	h_o (mm)	h_f (mm)	T (°C)	Reduction (%)
1	25.4	16.0	1.160	37
2	16.0	10.1	1.075	60
3	10.1	6.35	980	75

Cold Rolling
Laminado en Frío

Pass	h_o (mm)	h_f (mm)	Reduction (%)
1	6.1	4.3	30
2	4.3	3.1	50
3	3.1	2.0	67
4	2.0	1.5	75
5	1.5	1.12	81

transducer to obtain the orientation by EBSD. It is known that frictional forces at the metal and work-rolls interface affect the texture at the surface, which differs from that at the bulk of the sample. Hence, specimens of 25 mm by 20 mm by the thickness of the strip were polished by mechanical means until mid-thickness was reached; texture analyses were carried out on this surface.

A hydraulic machine was used for tension testing. The samples were an ASTM E8 standard (gage length 25.4 mm, width 6.25 mm, thickness 1.12 mm, length of reduced section 31.65 mm, radius of fillet 6.25 mm, overall length 101.4 mm) that were cut in directions parallel, perpendicular and 45° to the rolling direction. It was not possible to make duplicated tests due to the small amount of material available.

Mechanical properties such as yield strength (YP), ultimate tensile strength (UTS) and elongation (e %) were obtained by tension testing using samples parallel to the rolling direction. Normal anisotropy (r-value) and planar anisotropy (Δr) were obtained by means of:

$$r_m = (r_0 + 2r_{45} + r_{90}) / 4 \quad (1)$$

and

$$\Delta r = (r_0 - 2r_{45} + r_{90}) / 2 \quad (2)$$

Where **r** is given by the ration of strain along the width direction (ε_ω) to that along the thickness direction (ε_τ), after tensile deformation of about 15 percent, the subindex refers to the tests conducted on samples cut at 0,45 and 90° with respect to the rolling direction

3. RESULTS AND DISCUSSION

Cold rolled steel samples were annealed at different temperatures for 105 s, as this is the standard time used in continuous annealing[11]. Figure 1 shows the microhardness variation as a function of the annealing temperature. No recrystallization occurs below 600 °C, as the hardness remains constant, but between 600 and 750 °C the hardness decreases, which can be attributed to recovery. Recrystallization starts at 800 °C, when a maximum drop in hardness is achieved. An increase in hardness at 900 °C was detected. This phenomenon is originated as the alloy reaches the two-phase region caused by the gamma loop region of the Fe–Cr phase diagram, (Fig. 2) [12]. At this temperature austenite will be formed and will transform into martensite along ferrite grain boundaries during cooling. Two phases were identified by means of Vickers's microhardness indentation, which were ferrite and martensite. The figure 3 a) shows a sample of microstructure obtained at 900 °C. It can see incipient martensite in grain boundaries. Figure 3 b) shows a micro indentation in a martensite zone. Results of the micro hardness for the ferrite and martensite zones are HV = 130 and HV = 270

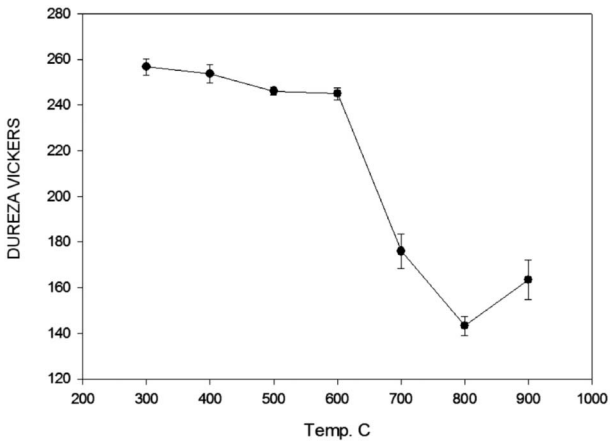

Figure 1. Annealing heat treatment at different temperatures for 105 s.

Figura 1. Tratamiento térmico de recocido a diferentes temperaturas por 105 s.

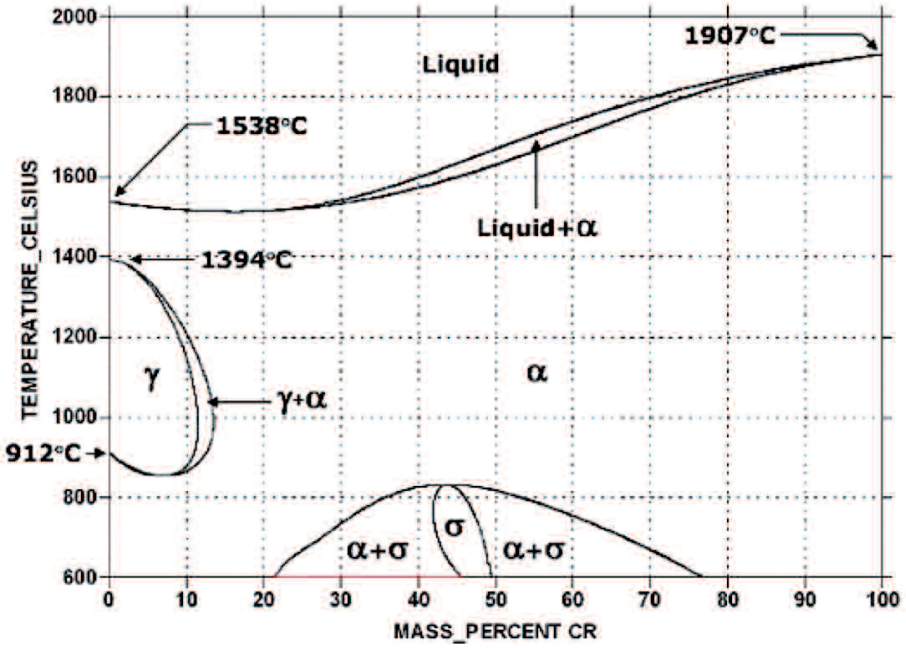

Figure 2. Cr-Fe phase diagram.

Figura 2. Diagrama de fases Cr-Fe.

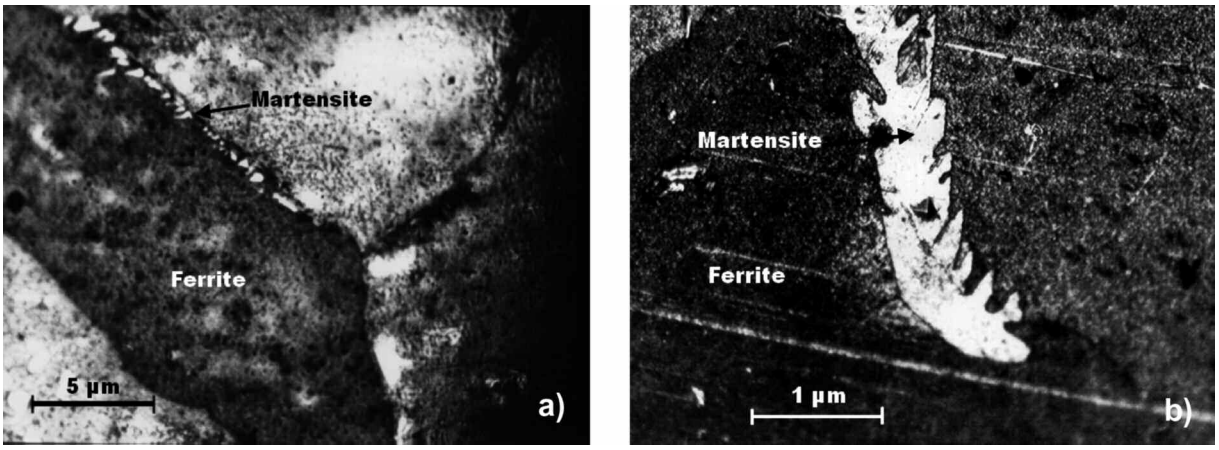

Figure 3. Microestructure of alloy annealed at 900 °C during 1.45 min (105 s): a) incipient martensite in grain boundaries, b) micro hardness indentation into a martensite zone.

Figura 3. Microestructura de la aleación recocida a 900 °C durante 1,45 min (105 s): a) inicio de formación de martensita en las fronteras de grano, b) Indentación de microdureza dentro

respectively. It is worth mentioning that the gamma loops varies according to the chemical composition, however for the current case it could be neglected. Changes in microstructure as function of annealing temperature are presented in figure 4. The early stages of recrystallization at 700 °C can be observed.

The steel after annealing at 800 °C for 105 s shows a microstructure with a large aspect ratio, which is defined as the ratio between the grain size measured on the longitudinal direction over the size measured along the transversal one (Table III). This ratio is related to the degree of recrystallization. Therefore, it was necessary to perform additional annealing treatments for longer times.

The alloy showed improved behavior when it was annealed for 14 min at 800, 850, and 900 °C. Grain

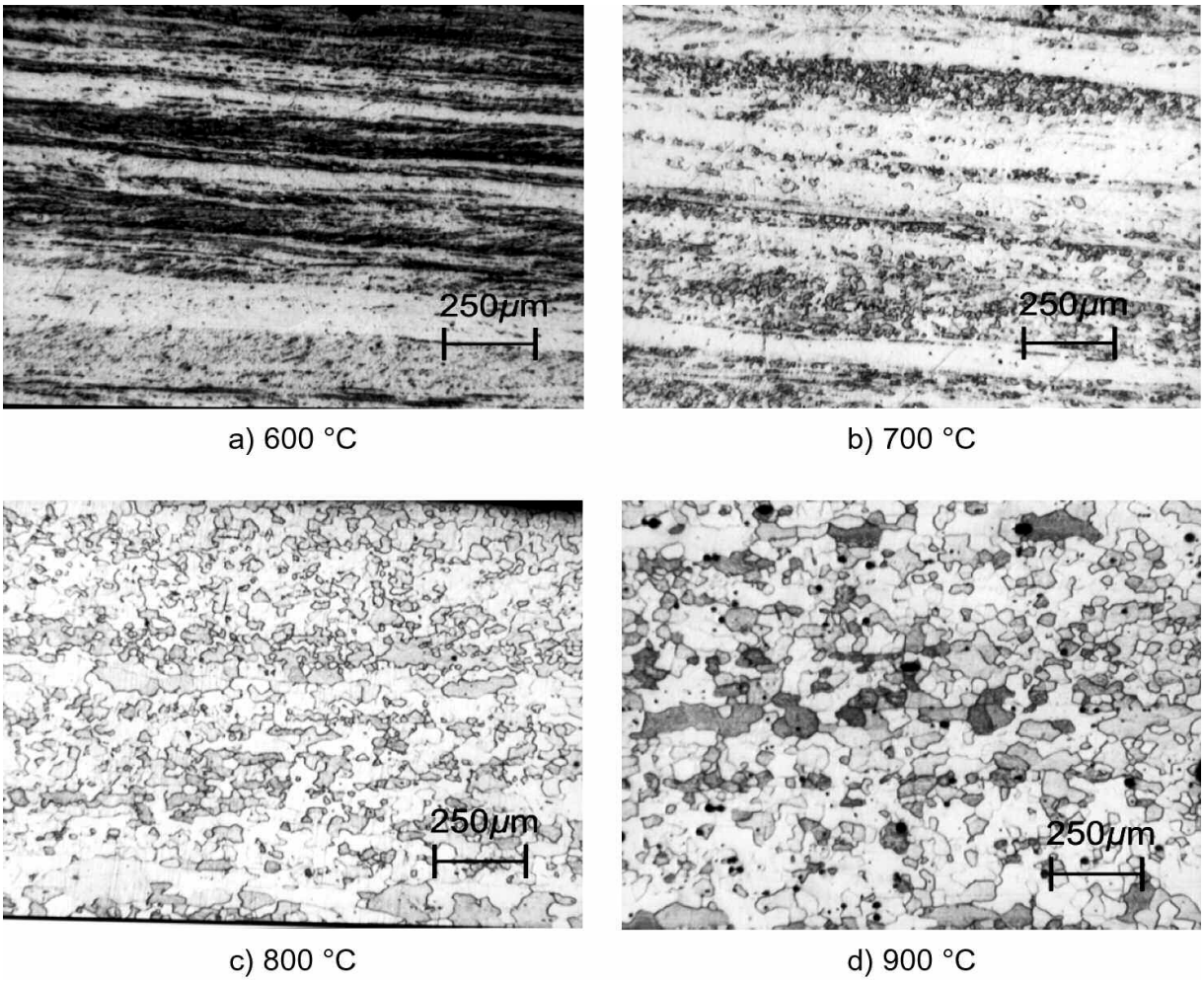

Figure 4. Microstructures of alloy at different temperatures of annealing during105 s (→Rolling Direction).

Figura 4. Microestructura de la aleación a diferentes temperaturas de recocido durante 105 s (→Dirección del laminado).

Table III. Average size (d) and aspect ratio after annealing for 105 s at 800 and 900 °C

Tabla III. Tamaño de grano (d) y razón de aspecto después del recocido por 105 s a 800 y 900 °C

800 °C		900 °C	
d (μm)	Aspect. ratio	d (μm)	Aspect. ratio
17.6 ± 13.1	1.62 ± 0.7	18.1 ± 9.6	1.44 ± 0.5

size increased marginally with temperature (Table IV), showing a smaller standard deviation than when the samples were annealed for 105 s, and smaller aspect ratio. These observations may be indicative that the alloy achieved complete recrystallization.

It can be considered that an alloy is fully recrystallized when almost the grains boundaries have a misorientation angle higher than 15°, which means that the grains are in their stable state. If the alloy is kept at a high temperature for longer times, the grain size will increase, a process that has been called abnormal grain growth or secondary recrystallization[13 and 14]. Care was taken to avoid this problem, as there was not time enough for such a phenomenon to take place, as the metallographic results indicate that the changes in grain size are kept within a small range.

When two grains have a misorientaion angle less than 15°, they can be in an unstable state, and are known as subgrains, with time and temperature; they will recrystallize by subgrain rotation and coalescence mechanisms.

An effective method of evaluating the degree of recrystallization in a given sample is to calculate the

Table IV. Average size (d) and aspect ratio after annealing for 14 min (840 s) at 800, 850 and 900 °C

Tabla IV. Tamaño de grano (d) y razón de aspecto después del recocido por 14 min (840 s) a 800, 850 y 900 °C

800 °C		850 °C		900 °C	
d (μm)	Aspect. ratio	d (μm)	Aspect. ratio	d (μm)	Aspect. ratio
15.31 ± 6.81	1.21 ± 0.04	15.81 ± 5.15	1.28 ± 0.02	16.64 ± 5.84	1.05 ± 0.01

volume fraction of recrystallized grains. There is an ideal grain boundary distribution whose frequency is random[15]. As the area fraction of grain boundary misorientation approaches the normal distribution, the volume fraction of recrystallized grains increases. Full recrystallization is achieved when both distributions are similar.

Figure 5 shows the area fraction of recrystallized grains annealed at 900 °C for different times versus random distribution. It shows that, with increasing time, the fraction area moves toward grain boundaries with higher misorentation, approaching a random distribution, which means that recrystallization increases with time. Table V shows the percentage of area fraction for the curves showed in figure 5. The

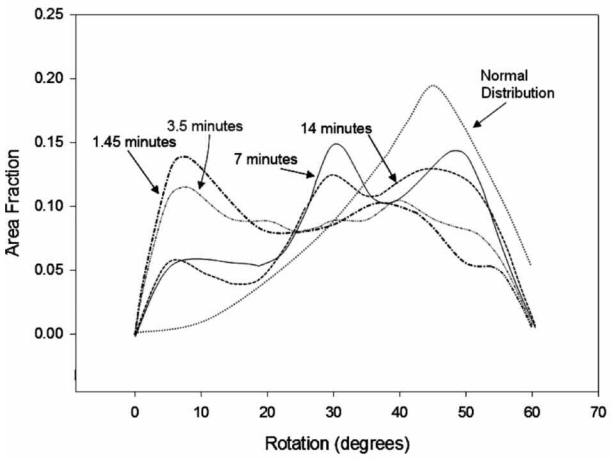

Figure 5. Comparison of the intensity of the grain boundary misorientation area fraction as function of constant temperature of 900 °C at different annealing times.

Figura 5. Comparación de la intensidad de la fracción de área de la desorientación de las fronteras de grano como función de temperatura constante a 900 °C para diferentes tiempos de recocido.

Table V. Area fraction of grain boundary misorientation of samples annealed at 900 °C and different times

Tabla V. Fracción de área de la desorientación de las fronteras de granos de muestra recocidas a 900 °C y diferentes tiempos

Time (min)	% Area fraction
1.45	61.9
3.5	66.4
7	79.7
14	80.6

condition of the highest recrystallization at 900 °C was found at a 14 min period.

Since the annealing at 14 min showed the optimum results, other tests were performed at different temperatures in order to find a higher recrystallization.

Figure 6 shows the area fraction of samples annealed for 14 min at different temperatures versus random distribution. It can be seen that the behavior between temperatures of 800 and 900 °C is almost the same, although, the results are better for 850 °C. Table VI shows the percentage of area fraction for the curves showed in figure 6. The alloy at 850 °C and at a period of 14 min time showed the best recrystallization.

Figures 7 and 8 (corresponding to {100} and {111} planes) show pole figures obtained from samples annealed at different temperatures for constant holding time (14 min). This test proves that at 850 °C the alloy has a very good fiber texture.

Figure 9 shows an ODF section at $\phi 2 = 45°$, Bunge notation, of the material annealed for 14 min at different temperatures. The diagrams indicate an improved gamma fiber texture in the samples annealed at 850 °C (Fig. 9 b)).

Table VI. Area fraction of grain boundary misorientation of samples annealed for 14 min at different temperatures

Tabla VI. Fracción de área de la desorientación de las fronteras de granos de muestra recocidas por 14 min a diferentes temperaturas

Temperature °C	% Area fraction
800	77.1
850	85.0
900	80.6

ASTM specifications (A 240) [16], for ferritic stainless steels 409 indicate that their minimum mechanical properties must be 205 MPa for yield stress, 380 MPa for ultimate tension stress, and 20 % of total elongation.

A major portion of ferritic stainless steel production is cold rolled into sheet. A very substantial

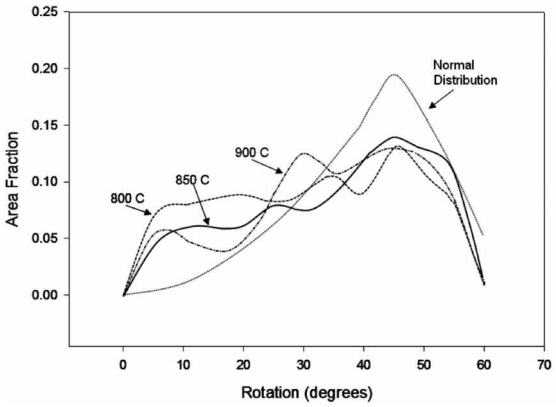

Figure 6. Comparison of the intensity of the grain boundary misorientation area fraction as function of different annealing temperature at constant time of 14 min (840 s).

Figura 6. Comparación de la intensidad de la fracción de área de la desorientación de las fronteras de grano en función de diferentes temperaturas de recocido a un tiempo constante de 14 min (840 s).

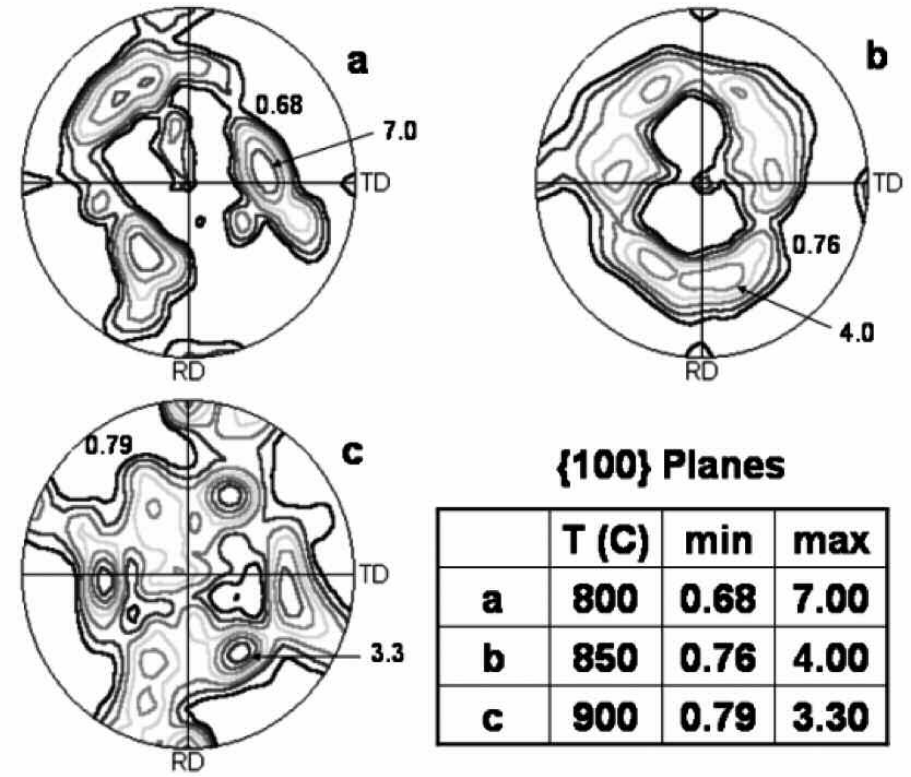

Figure 7. Resulting pole figures for alloy after annealing at different temperatures at constant holding time 14 min (840 s){100}.

Figura 7. Resultados de la figura de polos para la aleación después del recocido a diferentes temperaturas a tiempo constante de 14 min (840 s) {100}.

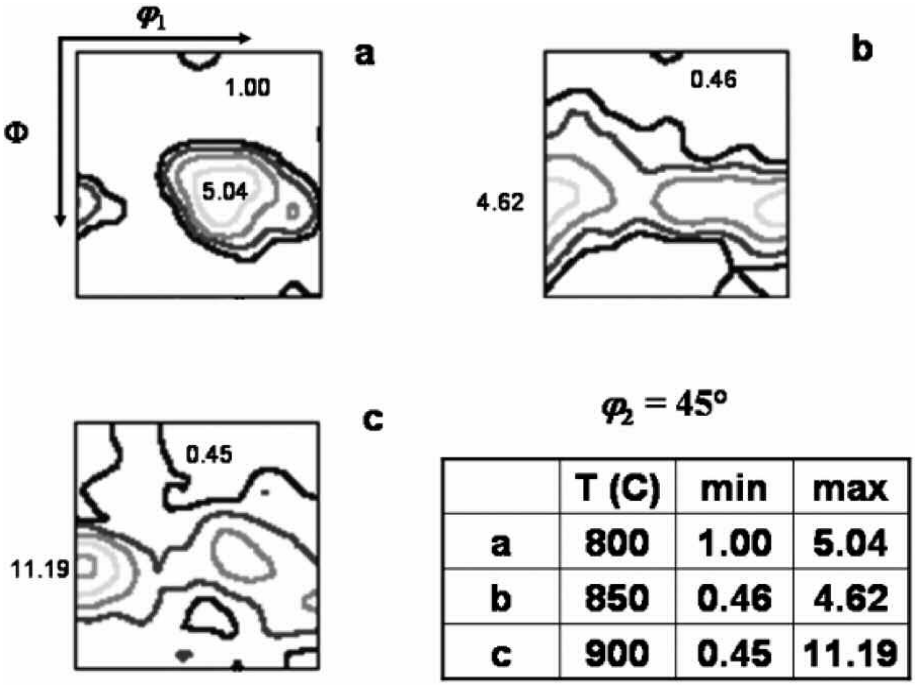

	T (C)	min	max
a	800	1.00	5.04
b	850	0.46	4.62
c	900	0.45	11.19

Figure 8. Resulting pole figures for alloy after annealing at different temperatures at constant holding time 14 min (840 s){111}.

Figura 8. Resultados de la figura de polos para la aleación después del recocido a diferentes temperaturas a tiempo constante de 14 min (840 s) {111}.

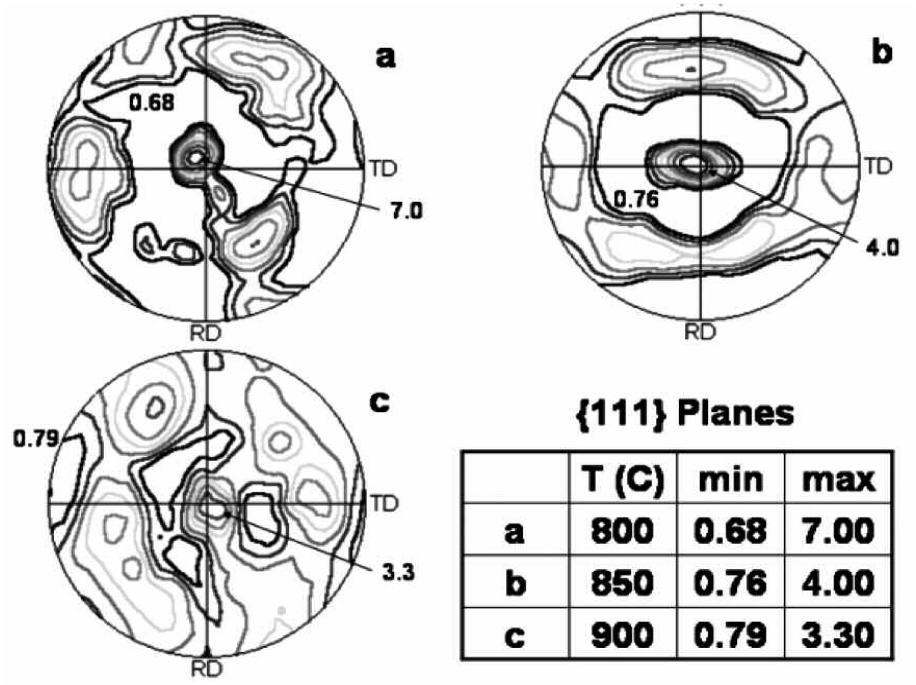

	T (C)	min	max
a	800	0.68	7.00
b	850	0.76	4.00
c	900	0.79	3.30

Figure 9. ODF section at $\phi 2 = 45^{\circ}$ of alloy annealing for 14 min (840 s), at different temperatures.

Figura 9. Sección de ODF a $\phi 2 = 45^{\circ}$ de la aleación recocida a 14 min (840 s) a diferentes temperaturas.

portion of this sheet is subsequently formed by deep drawing or stretch forming and thus good sheet formability is a very important property of ferritic stainless steels.

The mechanical properties of 409 ferritic stainless steel that support good sheet formability are low yield stress (YP), low ultimate tensile stress (UTS), high percent elongation (e%), normal anisotropy (r-value) greater than 1.5, and planar anisotropy (Dr) equal to zero[17].

Table VII presents the results of the mechanical properties of the samples investigated. Comparing the current results against the values obtained from the annealing standard, it has been noted that the mechanical properties (i.e. YS, UTS and e%) present similarities among all temperatures used during test. Nevertheless, it is important to find out among other properties such as anisotropy ($\mathbf{r_m}$) and texture, which can be the key properties influencing the improvement of the formability process (i.e. drawability or stretching).

Based on the current results the optimal formability properties were achieved after a 14 min period of annealing at 850 °C. It is due to its high value of planar anisotropy (Table VII) and also a high intensity ratio {111} /{100} and a strong fiber texture (Fig. 9 b)). Table VIII shows the texture influence on the r_m values. The higher the intensity, the higher the r_m values, it has been also reported in the case of other steels[18].

4. CONCLUSIONS

— The best annealing cycle for the stabilized ferritic stainless steel 409 with zirconium and titanium additions understudy was of 850 °C during 14 min. It is due to its high values of $\mathbf{r_m}$ and texture obtained.
— This annealing cycle allows the formation of a strong fiber texture which enhances the formability of the steel.
— The mechanical properties such as YS, UTS and e% present similar values in a range of 800 to 900 °C for a 14 min period. These values achieve the annealing standard.

Table VII. Mechanical properties after cold rolling and annealing for 14 min at different temperatures

Tabla VII. Propiedades mecánicas después del laminado en frío y recocido por 14 min (840 s) a diferentes temperaturas

	800 °C	850 °C	900 °C
YP (MPa)	260	270	235
UTS(MPa)	405	396	375
HV	134	146	123
% e	41	38	36
r_m	1.22	1.94	1.2
Δr	0.82	0.89	0.1

Table VIII. Texture and r_m values

Tabla VIII. Valores de Textura y r_m

Planes	800 °C	850 °C	900 °C
{111}/{100}	1.48	2.41	1.25
r_m	1.22	1.94	1.2

Acknowledgements

The authors acknowledge the advisory support provided by Professors I. C. Garcia and Q. J. DeArdo from University of Pittsburgh, and the financial support from Universidad Autónoma de Nuevo León, Paicyt and CONACYT.

REFERENCES

[1] M. Hua, C.I. Garcia, and A.J. DeArdo, *ISS 38th* Mechanical Working and Steel Processing Conference, Cleveland, EE.UU.,1997, pp. 41-44.
[2] Y. Inove and M. Kikucki, Nippon Steel Thecnical Report, Japan, Nº 88, July 2003, pp. 61-69.
[3] J. Rege, M.S.Thesis, Materials Science and Engineering, University of Pittsburgh, 1993.
[4] Y. Xu, C.I. Garcia, I. Franson, and A.J. DeArdo, International Symposium. On Low Carbon Steels for the 90's, R. Asfahani and G. Tither (Eds.) TMS, Warrendale, PA, 1993, pp. 397-404.
[5] S. D. Washko, and J.L. Grubb, Proceedings of International Conference on Stainless Steels, *ISIJ*, Chiba, Japan, June 10-13, 1991.
[6] J.L. Cavazos, *Materials Characterization*, Ed. Elsevier, 56 (2006) pp. 96-101.
[7] B.D Cullity, *Elements of X-ray Diffraction*, Ed. Addison-Wesley, 1977, pp. 295-321.

[8] I.L. Dillamore and W.T. Roberts, *Met. Rev. Madrid* 10 (1965) 271-380.
[9] F.A. Underwood, *Textures in Metals Sheets*, Ed. MacDonald, London, 1961.
[10] D.V.Wilson, *Met. Rev. Madrid* 139 (1969) 175-188.
[11] J. Rege, PhD Thesis Doctoral, University of Pittsburgh, EE.UU. 1998.
[12] E.C. Bain, and R.H. A. Chromium, *Iron Phase Diagram*, Metals Handbook, American Society for Metals, Metals Park, Ohio, EE.UU. 1948, p. 1194.
[13] J.J. Jonas and L. Kestens, Proc. of 1st Joint Int. Conf. on Recrystallization and Grain Growth, Ed. by G. Gottstein and D. A. Molodov, Springer-Verlag, Berlin, 2001, pp. 49-60.
[14] R.W. Cahn, Physical Metallurgy, 4 Edition, R.W. Cahn and P. Haasen (Eds.), Amsterdam, North Holland, 1996, pp. 2399-2500.
[15] J.K. Mackenzie: *Biometrika,* 45 (1958) p. 229.
[16] *ASTM A 240/A 240M* Standard Specification for Chromium and Chromium-Nickel Stainless Steel Plate, Sheet, and Strip for Pressure Vessels and for General Applications, 2009, pp. 9-13.
[17] ASM Handbook Volume 1, Tenth Edition, Rudolf Steiner and American Society for Metals, ASM International, Ohio, EE.UU., 1990, pp. 1330-1332.
[18] D. Raabe and K. Luucke, *Textures of ferritic stainless steels, Materials Science and Thechnology*, Ed. Maney Publishing, Vol. 9, 1993, pp. 302-312.